Proceedings of the Sixth International Conference on Research in Intelligent and Computing pp. 81–86
DOI: 10.15439/2021R16
ISSN 2300-5963 ACSIS, Vol. 27

LQR Controller Design for Mini Motion Package Electro-Hydraulic Actuator Control

NguyenVan Tan
School of Engineering – Technique Thu Dau Mot University Binh Duong, Vietnam
tannv@tdmu.edu.vn or 0000-0001-5929-6000

Huy Q. Tran*
Faculty of Engineering – Technology Nguyen Tat Thanh University Ho Chi Minh City, Vietnam
tqhuy@ntt.edu.vn

Phan Viet Hung
School of Engineering – Technique Thu Dau Mot University Binh Duong, Vietnam
hungpv@tdmu.edu.vn

Huynh Minh Phu
School of Engineering – Technique Thu Dau Mot University Binh Duong, Vietnam
phuhm@tdmu.edu.vn

***Abstract*—Electro-hydraulic actuators have been widely applied in the industry because they have several major advantages. In this paper, we focused on controlling the mini motion package electro-hydraulics actuator. First, a mathematical model of the electro-hydraulic actuator (EHA) was implemented to apply the control process to the proposed system. Second, we applied the linear quadratic regulator (LQR) controller to a linear model that is converted from the nonlinear EHA system. Finally, the numerical simulation results were performed in which the results obtained from the LQR controller were compared with the PID controller to show the superiority of the proposed solution.**

***Index Terms*—Linear control system; LQR controller; PID controller, Electro-hydraulics actuator.**

I. Introduction

IN THE past decades, different types of electro-hydraulic systems have been developed with different purposes for industrial systems, such as heavy-duty equipment and some machining equipment. These systems have many great advantages such as fast response, high control precision and high output power based on position, force and pressure control signals. It is considered one of the most promising choices for modern industry and has become an indispensable control method in mechanical manufacturing, construction machinery and defense. Moreover, the development of information technology has also greatly improved the quality of control process.

To improve the performance of the electro-hydraulic actuator (EHA) system, several EHA types were designed as shown in [1-3], and the use of conventional and advanced controllers to improve control accuracy, including proportional–integral–derivative (PID) controller [4-7], sliding mode controller and adaptive back-stepping ccontrol [8,9], has been studied. Recently, many researchers have been focused on new approaches, such as fault-tolerant control and fault-tolerant control compensation based on fault estimation using observer technology [4,10-12]. Research on linear quadratic regulator (LQR) controller were also implemented for the EHA system [13-15].

In this paper, an LQR controller is applied to control the linear EHA system. The gain K in the LQR controller is designed based on the algebraic Riccati Equation with the quadratic performance functional and the cost function. The cost function corresponding to R and Q is equally important for the control and the state variables as the output (piston position, piston velocity and piston acceleration). The controller can be tuned by varying the positive elements in the Q, R matrix to achieve the desired response. A PID controller is used for the numerical simulation process of the EHA system. The response signal in the LQR case is compared with the response signal in the PID case.

The important contributions of paper can be shortened as follows:

- The mathematical model of the EHA system was converted to the linear system for the application of this controller
- The gain K was calculated using Matlab software via Q, R matrices, the algebraic Riccati Equation with the quadratic performance functional, and the cost function
- A scale value factor N is also computed thanks to the EHA's parameters.
- The successful numerical simulation results of the EAH system was respectively presented.

II. EHA Model Formulation

The dynamics of EHA can be expressed the motion of the positioning piston via the mass of object M_p [4]:

$$m_p\ddot{\ell}_p + \Upsilon\dot{\ell}_p + F_{sp} + F_{frc} + \upsilon = S_1\Pi_1 - S_2\Pi_2 \qquad (1)$$

where m_p, $\ell_p, \dot{\ell}_p$ and $\ddot{\ell}_p$ are the mass, the position, the velocity, and the acceleration of object M_p respectively.

S_1,Π_1, and S_2,Π_2 are the area, the pressure in two chambers of the cylinder respectively.

F_{sp}, Υ, F_{frc}, and υ are the external load force of the spring impact on the piston, the viscosity damping

* corresponding author

coefficient, the friction force, and unknown disturbance respectively.

The spring force F_{sp} can be computed as:

$$F_{sp} = \delta_{sp}\ell_p \tag{2}$$

where δ_{sp} is the stiffness of the spring.

The friction force F_{frc} can be presented as [4]

$$F_{frc} = \sqrt{2e}\left(F_{brk} - F_C\right)e^{-\left(\frac{v_p}{v_{st}}\right)^2}\frac{v_p}{v_{st}} + F_C \tanh\left(\frac{v_p}{v_{cl}}\right) \tag{3}$$

where F_{brk}, F_C, and B_v are breakaway friction, Coulomb friction, and viscous friction coefficient, respectively. v_p, and v_{st} are position velocity, Stribeck velocity threshold.

The hydraulic continuity equations for the EHA system can be expressed as [4]:

$$\dot{\Pi}_1 = \varphi_1\left(\Phi_{1i} - S_1\dot{\ell}_p\right) \tag{4}$$

$$\dot{\Pi}_2 = \varphi_2\left(\Phi_{2i} + S_2\dot{\ell}_p\right) \tag{5}$$

$$\Phi_{pump} = \Delta_p\omega \tag{6}$$

where

$$\Phi_{13i} = \Phi_{pump} + \Phi_{1v} - \Phi_{3v} - \Phi_i$$
$$\Phi_{24i} = -\Phi_{pump} + \Phi_{2v} - \Phi_{4v} + \Phi_i$$

$$\varphi_1 = \frac{\beta_e}{\left(V_{01} + S_1\ell_p\right)}, \text{ and } \varphi_2 = \frac{\beta_e}{\left(V_{02} - S_2\ell_p\right)}$$

β_e, Φ_i, V_{01}, and V_{02} are the effective bulk modulus in each chamber, the internal leakage flow rate of the cylinder, the initial total control volumes of the first and the second chamber respectively [4].

$\Phi_{1v}, \Phi_{2v}, \Phi_{3v}, \Phi_{4v}$, and Φ_{pump} are the flow rate through the pilot operated check valve on the left, on the right, the flow rate through the pressure relief valve on the left, on the right, and the pump flow rate respectively. Δ_p, and ω are the displacement and the speed of the servo pump [4]

From equation (1) to (6) and the derivative both sides of equation (1), we have:

$$m_p\dddot{\ell}_p + \Psi\ddot{\ell}_p + \delta_{sp}\dot{\ell}_p = S_1\Pi_1 - S_2\Pi_2 \tag{7}$$

where

$$\Psi = -\frac{F_C}{v_{cl}}\tanh\left(\frac{\dot{x}_p}{v_{cl}}\right)^2 + \frac{\sqrt{2e}\left(F_{brk} - F_C\right)e^{-\left(\frac{\dot{x}_p}{v_{st}}\right)^2}}{v_{st}} - \frac{2\sqrt{2e}\dot{x}_p^2\left(F_{brk} - F_C\right)e^{-\left(\frac{\dot{x}_p}{v_{st}}\right)^2}}{v_{st}^3} + \frac{F_C}{v_{cl}} + \Upsilon$$

Substitution equation (4), (5) into (7), we obtain as:

$$\begin{aligned}\dddot{\ell}_p &= -\frac{\Psi}{m_p}\ddot{\ell}_p - \frac{\delta_{sp}}{m_p}\dot{\ell}_p + \frac{\left(S_1\varphi_1 + S_2\varphi_2\right)}{m_p}\Delta_p u - \frac{\left(S_1^2\varphi_1 + S_2^2\varphi_2\right)}{m_p}\dot{\ell}_p + \frac{\Omega}{m_p} \\ &= f\left(\ell, u\right)\end{aligned} \tag{8}$$

where

$$\Omega = S_1\varphi_1\Phi_{13i} - S_2\varphi_2\Phi_{24i}$$

Equation (8) can be written as

$$\dot{x} = f(x,u) \tag{9}$$

where

$x = \begin{bmatrix} x_1^T & x_2^T & x_3^T \end{bmatrix}$, and $x_1 = \ell_p; x_2 = \dot{\ell}_p; x_3 = \ddot{\ell}_p$

Equation (9), can be rewritten as

$$\begin{bmatrix}\dot{x}_1 \\ \dot{x}_2 \\ \dot{x}_3\end{bmatrix} = \begin{bmatrix} x_2 \\ x_3 \\ -\frac{\Psi}{m_p}\ddot{\ell}_p - \frac{\delta_{sp}}{m_p}\dot{\ell}_p + \Gamma_1\Delta_p u - \Gamma_2\dot{\ell}_p + \frac{\Omega}{m_p}\end{bmatrix} = \begin{bmatrix} f_1(x,u) \\ f_2(x,u) \\ f_3(x,u)\end{bmatrix} \tag{10}$$

$$\Gamma_1 = \frac{\left(S_1\varphi_1 + S_2\varphi_2\right)}{m_p}; \Gamma_2 = \frac{\left(S_1^2\varphi_1 + S_2^2\varphi_2\right)}{m_p}$$

The appropriate equation written in a state-space format of EHA system based on a Taylor expansion is given as:

$$\dot{x}(t) = Ax(t) + Bu(t) \tag{11}$$

where A, B matrices are calculated as:

$$A=\begin{bmatrix} a_{11} & a_{12} & a_{13} \\ a_{21} & a_{22} & a_{23} \\ a_{31} & a_{32} & a_{33} \end{bmatrix}; B=\begin{bmatrix} b_1 \\ b_2 \\ b_3 \end{bmatrix};\ u=\omega$$

where the parameters of the EHA system are provided in Table 1

Table 1. Basic parameters of the EHA system.

Parameters	Symbols	Values	Units
Piston cross-sectional area on the left	S_1	0.0013	m^2
Piston cross-sectional area on the right	S_2	$9.4\ 10^{-4}$	m^2
The initial total control volumes on the left	V_{01}	$2.09\ 10^{-4}$	m^3
The initial total control volumes on the right	V_{02}	$4.006\ 10^{-5}$	m^3
Mass of the control object	m_p	10	kg
Bulk Modulus	β_e	$2.9\ 10^{8}$	Pa
The stiffness of the spring	δ_{sp}	2383	Nm
The displacement of the servo pump	Δ_p	$3.5\ 10^{-6}$	m^3

The elements of matrix B is computed as:

$$b_1=\frac{\partial f_1(x,u)}{\partial u};\quad b_2=\frac{\partial f_2(x,u)}{\partial u};$$

$$b_3=\frac{\partial f_3(x,u)}{\partial u}=\frac{S_1^2\beta_e}{V_{01}+S_1x_1}+\frac{S_2^2\beta_e}{V_{02}-S_2x_1}$$

The elements of matrix A is computed as:

$$a_{11}=\frac{\partial f_1(x,u)}{\partial x_1}=0;\quad a_{12}=\frac{\partial f_1(x,u)}{\partial x_2}=1;\quad a_{13}=\frac{\partial f_1(x,u)}{\partial x_3}=0$$

$$a_{21}=\frac{\partial f_2(x,u)}{\partial x_1}=0;\quad a_{12}=\frac{\partial f_2(x,u)}{\partial x_2}=0;\quad a_{13}=\frac{\partial f_2(x,u)}{\partial x_3}=1$$

$$a_{31}=\left.\frac{\partial f_3(x,u)}{\partial x_1}\right|_{\substack{x_1=0\\x_2=0\\u=0}}$$

$$=\left.\left(\frac{S_1^2\beta_e}{\left(V_{01}+S_1x_1\right)^2}-\frac{S_2^2\beta_e}{\left(V_{02}-S_2x_1\right)^2}\right)x_2\right|_{\substack{x_1=0\\x_2=0\\u=0}}$$

$$-\left.\left(\frac{S_1^3\beta_e}{\left(V_{01}+S_1x_1\right)^2}-\frac{S_2^3\beta_e}{\left(V_{02}-S_2x_1\right)^2}\right)*u\right|_{\substack{x_1=0\\x_2=0\\u=0}}$$

$$a_{32}=\frac{\partial f_3(x,u)}{\partial x_2}$$

$$=\left(\frac{2F_c tanh\left(\frac{x_2}{v_{cl}}\right)\left(tanh\left(\frac{x_2}{v_{cl}}\right)^2-1\right)}{{v_{cl}}^2}\right)x_3-6\sqrt{2e}\,e^{-\left(\frac{x_2}{v_{st}}\right)^2}\left(\frac{F_{brk}-F_c}{v_{st}^3}\right)x_2$$

$$\left.+4\sqrt{2e}e^{-\left(\frac{x_2}{v_{st}}\right)^2}\left(\frac{F_{brk}-F_c}{v_{st}^5}\right){x_2}^3-\gamma_2-\frac{S_1\beta_e}{V_{01}+S_1x_1}-\frac{S_2\beta_e}{V_{02}-S_2x_1}\right|_{\substack{x_1=0\\x_2=0\\u=0}}$$

$$a_{33}=\frac{\partial f_3(x,u)}{\partial x_3}$$

$$\left.=\sqrt{2e}\,e^{-\left(\frac{x_2}{v_{st}}\right)^2}\frac{F_{brk}-F_C}{v_{st}}-\frac{F_C\left(tanh\left(\frac{x_2}{v_{cl}}\right)^2-1\right)}{v_{cl}}-\gamma_1\right|_{\substack{x_1=0\\x_2=0\\u=0}}$$

$$\left.-(2\sqrt{2e}\,e^{-\left(\frac{x_2}{v_{st}}\right)^2}\left(\frac{F_{brk}-F_C}{v_{st}^3}\right)x_2^2\right|_{\substack{x_1=0\\x_2=0\\u=0}}$$

III. LQR CONTROLLER DESIGN

LQR is a powerful method for designing controllers based on the optimal algorithm that minimizes a given cost function. The parameter of the cost function is determined by two matrices Q and R which is calculated via the algebraic Riccati Equation with the quadratic performance functional and the cost function (12):

$$J(K)=\frac{1}{2}\int_0^\infty\left(x^T(t)Qx(t)+u^T(t)Ru(t)\right)dt \tag{12}$$

The optimal control signal is represented as

$$u^*(t)=-Kx(t) \tag{13}$$

Gain K is described as (14)

$$K=R^{-1}B^TP \tag{14}$$

where P is determined by the algebraic Riccati Equation (15):

$$PA+A^TP+Q-PBR^{-1}B^TP=0 \tag{15}$$

The state-space feedback Equation (16) can be built as shown in Fig. 1.

$$\begin{cases}\dot{x}(t)=Ax(t)+Bu(t)\\ y(t)=Cx(t)+Du(t)\end{cases} \tag{16}$$

We choose matrices C, and D is shown as:

$$C = I_{3\times3}; D = 0 \tag{17}$$

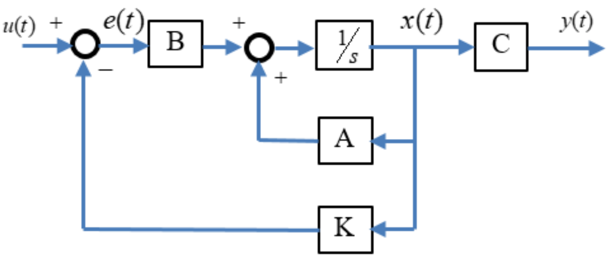

Fig. 1. Scheme diagram of the EHA system in state-space

Finally, matrices Q and R can choose as:

$$Q = C^T C = I_{3\times3} \ ; \ R = 1 \tag{18}$$

IV. Simulation Results

The obtained results from the simulation process of the EHA system with parameters (Table 1) are shown in Table 2 to verify the effectiveness of the suggested techniques. The numerical simulation processes are carried out and then the performance comparison between LQR and PID controllers with the input u(t) =0.2*ones(size(t)) was drawn.

First, simulation of the EHA system is done by the LQR controller with chosen matrices Q and R. Step response of piston position and velocity position are shown in Fig. 2.

$Q = I_{3\times3}$; and R = 1 and gain: K_1 =[1.000008 1.5746 10^{-3} 0.1]

Then, we continued obtain other simulations for cases 2, 3, and 4 in Table 2. These cases correspond to figures 3, 4, 5, respectively.

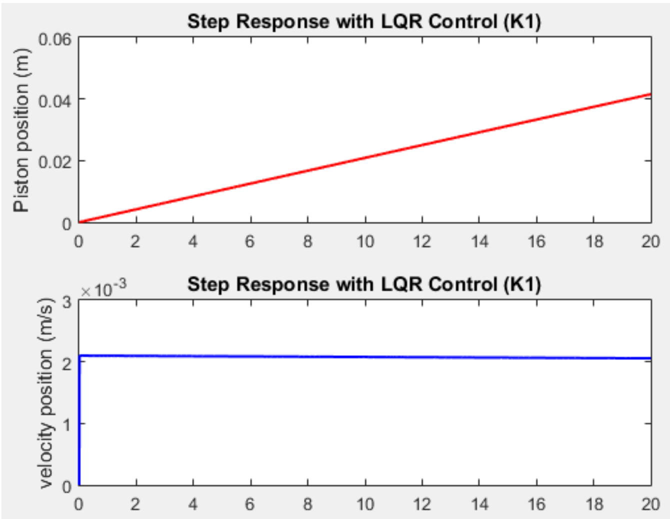

Fig. 2. Position and velocity response with LQR controller (K_1)

Table 2. Experimental results.

Cases	K, Q, R, N	Status	Setting time (s)
1	$Q = I_{3\times3}$; R=1, N=1 K_1 =1.0000008; 1.5746 10^{-3} ; 0.1	Unstable	None
2	$Q = 100000.I_{3\times3}$; R=1, N=1 K_2 =316.2278 146.2361 316.2275	Stable	18
3	$Q = \begin{bmatrix} 100000 & 0 & 0 \\ 0 & 0.001 & 0 \\ 0 & 0 & 0.005 \end{bmatrix}$ R = 0.005; N = 4.472 10^{3} K_3 = 4.472 10^{3} ; 4.683; 0.9997527	Stable	1.35
4	$Q = \begin{bmatrix} 100000 & 0 & 0 \\ 0 & 0.005 & 0 \\ 0 & 0 & 0.005 \end{bmatrix}$ R = 0.0001; N = 3.16 10^{4} K_4 = 3.162 10^{4} ; 211.316; 7.0708	Stable	0.25

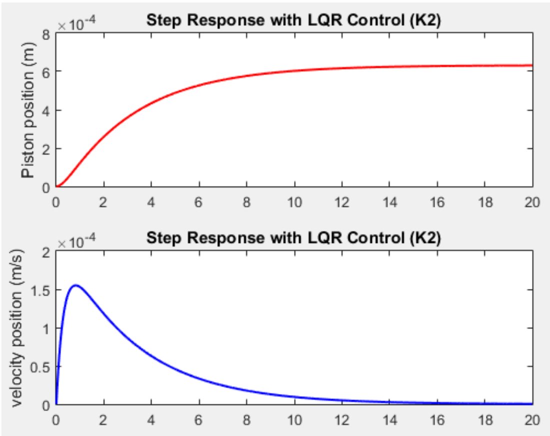

Fig. 3. Position and velocity response with LQR controller (K_2)

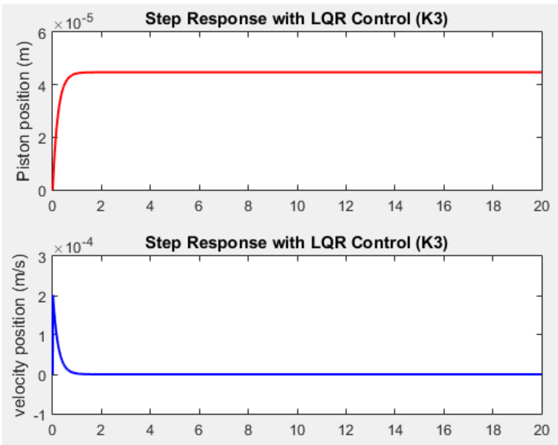

Fig. 4. Position and velocity response with LQR controller (K_3)

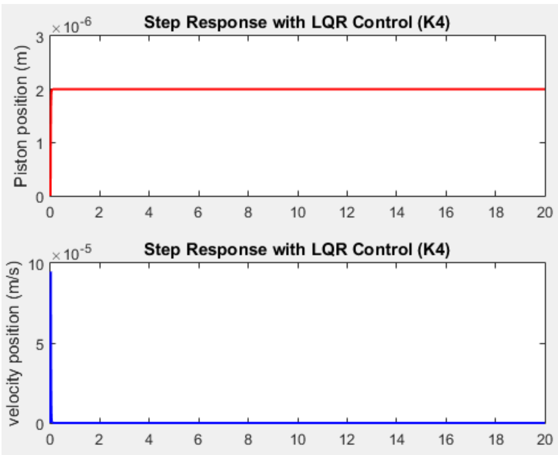

Fig. 5. Position and velocity response with LQR controller (K_4)

The scheme diagram of the EHA model in Simulink with N factor using the LQR controller can be described in Fig. 6. The simulation result in the third case is shown in Fig. 7 which is compared with position response for case without change (K_{p}.= *27.52272; K_I = 148.0119; K_D = 0.2*) in the PID controller.

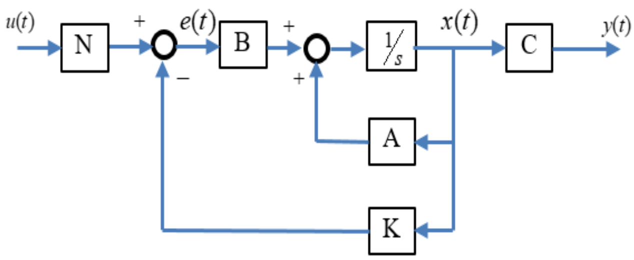

Fig. 6. Scheme diagram of the EHA system in state-space

The simulation results in the fourth case shown in Fig. 8 which is also compared with position response for case without change (K_{p}.= *27.52272; K_I = 148.0119; K_D = 0.2*) in the PID controller.

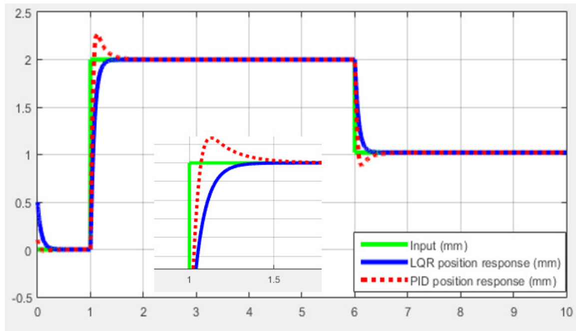

Fig. 7. Position and velocity response with LQR controller (K_3)

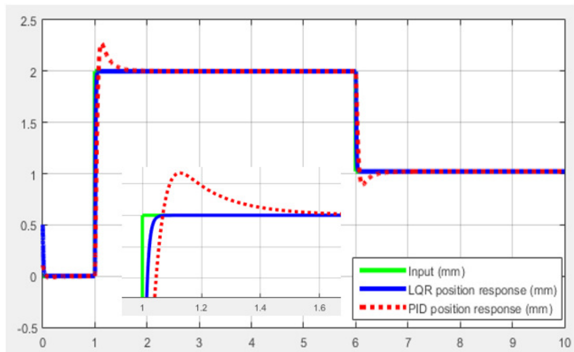

Fig. 8 Position and velocity response with LQR and PID controller (K_4)

In summary, the simulation results in the first case shown unstable position and velocity responses as shown in Fig. 2. In the second case (Fig. 3), the response is more stable when the Q value increases. The third and fourth cases showed the great effect of the Q and R parameters through the obtained response signal as illustrated in Fig. 4 and Fig. 5. We also see this influence in Fig.7 and Fig.8. These figures shown the superiority of the proposed controller thanks to achieved position responses.

V. CONCLUSIONS

The numerical simulation when applying the LQR controller show that the feedback signal of piston position in the EHA system achieved the expected results compared to the PID controller. The overshoot of the PID controller is greatly reduced and the response tim e of the feedback signal is also improved as shown in the previous section. However, to achieve the desired control signal when using an LQR controller, it is important to be experienced in the selection of parameters Q, R and parameter N.

Acknowledgment

This research was supported by Research Foundation funded by Thu Dau Mot University.

References

[1] Gabriele . A, Andrea . V, "A design solution for efficient and compact electro-hydraulic actuators", ScienceDirect, Procedia Engineering 106 (**2015**) 8 – 16

[2] Juliang . X , Qinyu . L, and et al "Theoretical and Experimental Analysis of the Hydraulic Actuator Used in the Active Reflector System" *Hindawi Mathematical Problems in* Engineering. Volume ***2018****, Article ID 8503628, 13 pages, doi.org/10.1155/2018/8503628*

[3] Shaoyang . Q, David . F, and et al "A Closed Circuit Electro-Hydraulics Actuator with Energy Recuperation Capability", *Novel system solutions, 12th International Fluid Power Conference, Dresden* ***(2020)***

[4] Tan, N. V.; and Cheolkeun, H.; "Experimental Study of Sensor Fault-Tolerant Control for an Electro-Hydraulic Actuator Based on a Robust Nonlinear Observer". *Energies,* MDPI, Open Access Journal, Energies (**2019)**, 12, 4337; doi:10.3390/en12224337

[5] Tan, V. N.; and Cheolkuen, H.; "The Actuator and Sensor Fault Estimation Using Robust Observer Based Reconstruction for Mini Motion Package Electro-Hydraulic Actuator". *Intelligent Computing Methodologies, Proceeding of 15th International Conference, ICIC 2019.* Nanchang, China, August 3–6. Part III, Pp. 244-256. (**2019)**.

[6] Norlela . I, Mazidah . T, and et al, "PID Studies on Position Tracking Control of an Electro-Hydraulic Actuator", *International Journal of Control Science and Engineering* ***2012****, 2(5): 120-126, DOI: 10.5923/j.control.20120205.04*

[7] Skarpetis .M. G, and Koumboulis. F. N, "Robust PID controller for electro — Hydraulic actuators," *2013 IEEE 18th Conference on Emerging Technologies & Factory Automation (ETFA)*, Cagliari, Italy, (**2013)**, pp. 1-5, doi: 10.1109/ETFA.2013.6648165.

[8] Ahn, K.K.; Nam, C.N.D.; Jin, M. Adaptive Back-stepping Control of an Electrohydraulic Actuator. *IEEE/ASME Trans. Mechatron.* **(2014)**, *19*, 987–995.

[9] Thomas. A. T, Parameshwaran. R, and et al "Improved Position Tracking Performance of Electro-Hydraulic Actuator Using PID and Sliding Mode Controller", *IETE Journal of Research*, (2019), DOI: 10.1080/03772063.2019.1664341

[10] Ahian, S.A., Truong, D.Q., Chowdhury, P. et al. Modeling and fault-tolerant control of an electro-hydraulic actuator. Int. J. Precis. Eng. Manuf. 17, 1285–1297 **(2016).** https://doi.org/10.1007/s12541-016-0153-2

[11] Mahulkar .V, Adams D. E, and Derriso .M, "Adaptive fault-tolerant control for hydraulic actuators," *2015 American Control Conference (ACC)*, Chicago, IL, USA, **(2015)**, pp. 2242-2247, doi: 10.1109/ACC.2015.7171066.

[12] Phan .V. D, Vo .C. P., Dao .H. V. and Ahn .K. K., "Robust Fault-Tolerant Control of an Electro-Hydraulic Actuator With a Novel Nonlinear Unknown Input Observer," *in IEEE Access*, vol. 9, pp. 30750-30760, 2021, doi: 10.1109/ACCESS.2021.3059947.

[13] Pourebrahim .M, Ghafari ,A. S, and Pourebrahim .M, "Designing a LQR controller for an electro-hydraulic-actuated-clutch model," *2016 2nd International Conference on Control Science and Systems Engineering (ICCSSE)*, Singapore, (**2016**), pp. 82-87, doi: 10.1109/CCSSE.2016.7784358.

[14] Tan .V .V, Olivier .S, Luc .D, Enhancing roll stability of heavy vehicle by LQR active anti-roll bar control using electronic servo-valve hydraulic actuators. Vehicle System Dynamics, Taylor & Francis, (**2017**), 55 (9), pp.1405-1429. Doi: 10.1080/00423114.2017.1317822.

[15] Priyanka .E, Maheswari .C, Thangavel .S. "Remote monitoring and control of LQR-PI controller parameters for an oil pipeline transport system". *Proceedings of the Institution of Mechanical eers, Part I: Journal of Systems and Control Engineering*. **(2019)**; 233(6):597-608. doi:10.1177/0959651818803183